Bulg. J. Phys. **42** (2015) 319–327

Density Functional Theory and Nuclear Shape Transitions

P. Ring
Physik Department, Technische Universität München,
85748 Garching, Germany

Received *15 October 2015*

Abstract. Covariant density functional theory beyond mean field is used to describe the collective dynamics of finite nuclei in terms of deformation degrees of freedom. As an example we show that the symmetry $X(5)$ of the quantum phase transition (QPT) between the $U(5)$ and the $SU(3)$ limits of the interacting boson model can be reproduced well within the relativistic version of the Generator Coordinate Method (GCM). This method is numerically very complicated and practically applicable only for very simple systems. The microscopic derivation of a collective Hamiltonian in five dimensions (5DCH) provides an elegant and simple alternative. We discuss benchmark calculations for the nucleus ^{76}Kr which show that there is very good agreement between both methods.

PACS codes: 21.60.Jz, 21.10.Re, 21.10.Tg, 27.50.+e

1 Introduction

Since the beginning of the century renewed interest has grown in experimental as well as in theoretical investigations for the study of nuclear dynamics in terms of shape degrees of freedom. Nuclear shape phase transitions have been the subject of a number of theoretical and experimental studies, pioneered by Iachello [1] and Casten and Zamfir [2]. These transitions can for instance be described in the geometric framework in terms of a Bohr Hamiltonian for shape variables, and related to the concept of critical symmetries which provide parameter independent (up to overall scale factors) predictions for excitation spectra and electric quadrupole (E2) transition rates for nuclei at the phase transition point [1]. The shape phase transition is accessed by variation of a control parameter, usually a parameter of the corresponding phenomenological Hamiltonian. Analytic solutions of the eigenvalue problem at the critical point correspond to a particular (critical) symmetry of the Hamiltonian.

Of course, nuclei consist of strongly interacting particles, protons and neutrons and nuclear shapes are in the strict sense no observables. It is therefore an important question whether nuclear QPTs can also be described in a general

microscopic framework. Covariant density functional theory (CDFT) provides an elegant and simple tool for such a purpose. It exploits basic properties of QCD at low energies, in particular, symmetries and the separation of scales [3]. Spin degrees of freedom are treated in a consistent way. CDFT also include the complicated interplay between the large Lorentz scalar and vector self-energies induced on the QCD level by the in medium changes of the scalar and vector quark condensates [4]. At present, all attempts to derive these functionals directly from the bare forces do not reach the required accuracy, but by fine tuning a few phenomenological parameters to properties of nuclear matter and finite nuclei, universal density functionals have been derived in recent years which provide an excellent description of ground states over the periodic table with a high predictive power [5].

On the other side, density functional theory is based on the concept of mean field theory. Symmetries are violated and nuclear spectra are not accessible in the simplest versions of DFT. In this contribution we therefore discuss methods to go beyond mean field theory and to calculate also low-lying nuclear spectra connected with shape degrees of freedom. This is in the first place the generator coordinate method (GCM) in connection with exact projection onto the subspaces of given symmetries. In Section 2 we discuss this method and show recent applications for the phase transition from spherical vibrators to axially symmetric rotors with the critical symmetry $X(5)$ at the transition point between these two limits. Unfortunately, GCM calculations are connected with a tremendous numerical effort. Therefore we show in Section 3 how such calculations can be simplified considerably by introducing a five-dimensional collective Hamiltonian (5DCH) in the shape degrees of freedom. The derivation of such a Hamiltonian is connected with additional approximations valid, in principle, only for rather heavy systems. It is therefore not clear whether the results obtained in this way are reliable. In Section 4 we therefore discuss recent benchmark tests comparing both methods for the same medium heavy nucleus ^{76}Kr.

2 The Relativistic GCM-Method for a Microscopic Description of Quantum Phase Transitions

The relativistic GCM has been discussed extensively in the recent literature [7, 8]. The starting point is a Lorentz invariant Lagrangian. Because of the complexity of the subsequent calculations point-coupling models have been used [9, 10]. In a first step fully self-consistent constrained relativistic mean field (RMF) calculations are carried out. Pairing correlations are treated in the BCS approximation. The constrained quantities depend on the problem under investigation. In the earlier investigations [6, 11] only axially symmetric β-deformations have been considered, i.e. the constraining operator was the mass quadrupole moment $\langle Q_{20}\rangle$, later also two constraining operators $\langle Q_{20}\rangle$ and $\langle Q_{22}\rangle$ [12,13] with the shape variables β and γ or $\langle Q_{20}\rangle$ and $\langle Q_{30}\rangle$ [14] with the

shape variables β_2 and β_3 have been taken into account. All the mean-field states are subsequently projected onto designed particle numbers N abd Z and angular momentum J by introducing the techniques of both particle number projection (PNP) and three-dimensional angular momentum projection (3DAMP) [7]. In the GCM method the shape fluctuations about the mean-field solution are determined variationally by mixing all the projected states in the Hill-Wheeler integral [15,16]. This level of implementation has become a standard and the state of the art microscopic model for studying nuclear low-lying collective excitations in the framework of relativistic [8, 12, 13] and non-relativistic DFT [17–20].

The nuclear many-body wave function is given as a linear combination of projected mean-field configurations generated by the collective coordinates of quadrupole deformations

$$|JNZ;\alpha\rangle = \sum_{q,K} f_{\alpha}^{JK}(q)\hat{P}_{MK}^{J}\hat{P}^{N}\hat{P}^{Z}|q\rangle\,, \tag{1}$$

where $\alpha = 1, 2, \ldots$ distinguishes different collective states with the same angular momentum J, and $|q\rangle = |\beta, \gamma\rangle$ denotes a set of RMF+BCS states with deformation parameters (β, γ). The operators $\hat{P}^N$, $\hat{P}^Z$, and $\hat{P}^J_{MK}$ project onto good particle numbers and angular momentum [16]. The weight coefficients $f_{\alpha}^{JK}(q)$ are determined by solving the Hill-Wheeler-Griffin equations [15, 21] that are deduced from the minimization of the energy. The solution of these equations provides the energy levels and all the information needed for calculating the electric multipole transition strengths [12].

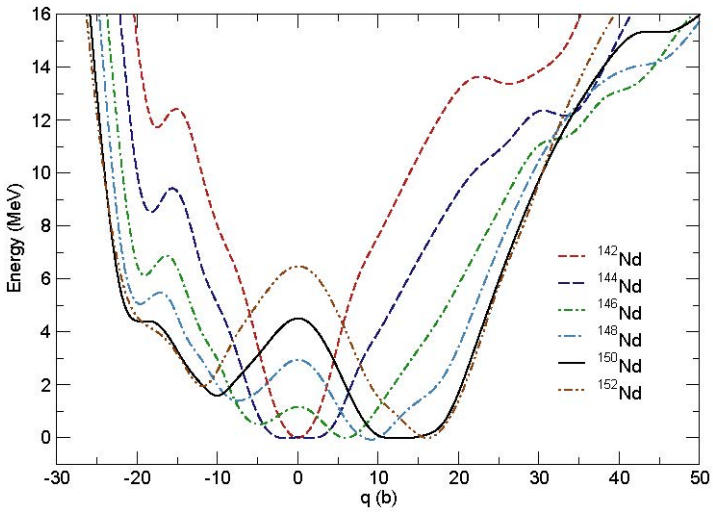

Figure 1. (Color online) Self-consistent RMF binding energy surfaces for the nuclei $^{142-152}$Nd as functions of the mass quadrupole moment q (from Ref. [6]).

In the following we discuss the phase transition from spherical to axially deformed shapes for the chain of Nd-isotopes. Using the Lagrangian PC-F1 [9] we show in Figure 1 the self-consistent mean field binding energy curves as functions of the mass quadrupole moment. These potential energy curves (PECs) display a gradual transition between the spherical nucleus ^{142}Nd and the strongly prolate deformed nucleus ^{152}Nd. The PEC of ^{150}Nd exhibits a wide flat minimum on the prolate side. One notes the similarity between the microscopic PEC shown in Figure. 1 and the original square well $X(5)$ potential considered in Ref. [1].

In Figure 2 the GCM results for the two lowest bands in ^{150}Nd are compared with data [22], and with the $X(5)$-symmetry predictions for the energies and $B(E2)$ values. In the mean-field plus GCM approach the transition rates are calculated in the full configuration space using bare charges, and the $B(E2)$ values can be directly compared with data. We note the excellent agreement of the GCM spectrum both with the data and with the $B(E2)$-symmetry predictions.

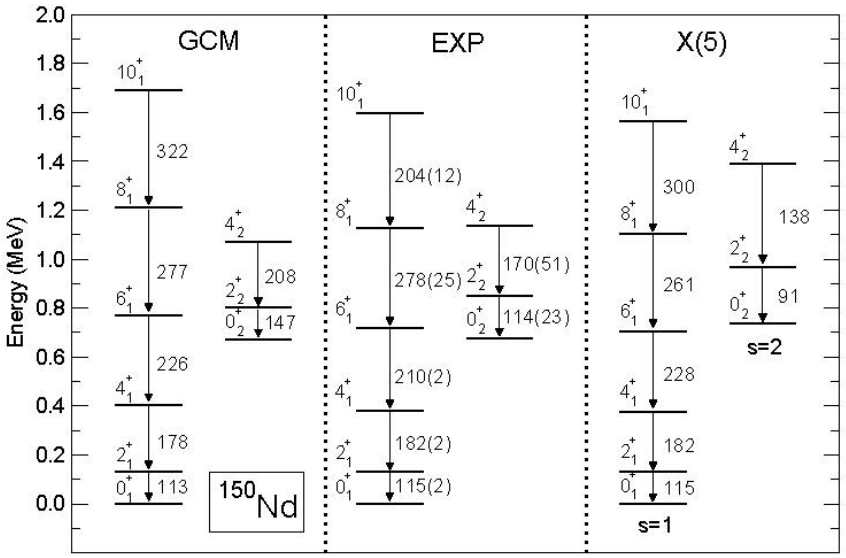

Figure 2. The low-lying part of the spectrum of the transitional nucleus ^{150}Nd: particle number and angular momentum projected GCM (left panel), experiment [22] (middle panel), and the prediction of the symmetry group $X(5)$ (right panel). The intraband and interband $B(E2)$ values of the ground state ($s = 1$) and the β ($s = 2$) bands are given in Weisskopf units. The theoretical spectra are normalized to the experimental energy of the state 2_1^+, and the $X(5)$ transition strengths are normalized to the experimental $B(E2; 2_1^+ \rightarrow 0_1^+)$ values (from Ref. [6]).

3 The Microscopic Derivation of a Collective Hamiltonian

Full GCM-calculations are connected with extreme numerical efforts. Full calculations with the two shape degrees of freedom β and γ and projection on angular momentum and particle number require the evaluation of a 7-dimensional integral. For each point in the integral a large complex matrix with the dimension of the underlying configuration space of overlap integrals has to be evaluated and inverted [16]. By this reason, even with modern supercomputers full 7D GCM calculations are at present only possible for relatively light nuclei. Heavy nuclei can, so far, only be treated with the restriction of axial symmetry (as in Figure 2).

On the other side, there are approximate methods. Since the seventies it is known [23, 24] that starting, from a microscopic Hamiltonian, it is possible to derive in the quadrupole case a collective Hamiltonian in the five shape degrees of freedom (5DCH) as it has first been introduced in a phenomenological way by Bohr [25, 26]. It contains an inertia tensor whose elements depend on deformation and a potential energy containing the full mean field energy and in addition several correction terms [27, 28]. This Bohr Hamiltonian has been derived in the literature from the microscopic theory in two rather different ways, (i) from the generator coordinate method (GCM) [23, 29–31] and (ii) from time-dependent Hartree-Fock (TDHF) theory [24, 32–34]. In both cases additional approximations had to be used.

A 5DCH has been derived in Ref. [35] for the quantum phase transition in the Nd-isotopes discussed in the last section. In this case triaxial deformations could be easily taken into account and the results are in very good agreement with axial GCM calculations shown in Figure 2. This is easy to understand by the fact, that in all cases the collective wave functions are centered around axial symmetry.

4 Benchmark Calculations in the Nucleus ^{76}Kr

Since the phase transition in the Nd-isotopes involves essentially only axially symmetric configurations, and since, in this case, the GCM calculations have been restricted to axial symmetry, this example cannot really serve as a critical test for the validity and usefulness of the 5DCH. In order to answer this question one has to consider a nucleus containing full triaxial configurations. In addition one has to carry out full triaxial GCM calculations together with the investigations using the corresponding collective Hamiltonian. Recently such a full benchmark calculation has been carried out in Ref. [13] for the nucleus ^{76}Kr with the relativistic point-coupling Lagrangian PC-PK1 [10].

Figure 3 displays various potential energy surfaces in the (β, γ) plane for ^{76}Kr. Panel (a) shows the mean field energy surface. A spherical minimum in the energy surface is found, soft along oblate shapes and competing with a large prolate deformed minimum. In panel (b) collective potential $V_{\rm coll}$ with zero-

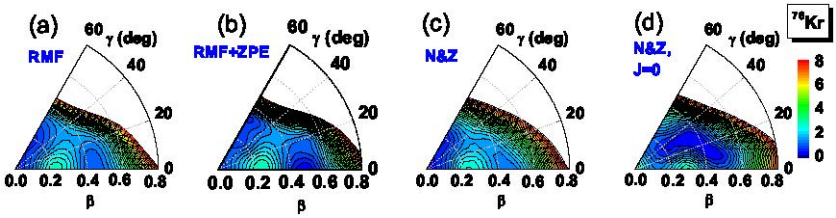

Figure 3. (Color online) Potential energy surfaces in the (β, γ) plane for ^{76}Kr: (a) constrained RMF+BCS, (b) RMF+BCS with zero-point corrections, (c) with PNP, and (d) with both PNP and 3DAMP ($J = 0$). Two neighboring contour lines are separated by 0.25 MeV (from Ref. [13]).

point corrections used in the 5DCH method is shown. These corrections do not change the energy surface in a qualitative way. Panel (c) displays the energy surfaces obtained from wave functions with exact particle number projection (PNP) after the variation and panel (d) with additional three-dimensional AMP. PNP alone does not lead to large deviations from the mean field surface, but 3DAMP changes the picture considerably. We observe a triaxial minimum, as it has been found in early triaxial projections in the rare earth region [36].

Figure 4 displays the low-lying spectra of ^{76}Kr. The full projected GCM calculation is compared with the experimental data and with results of the 5DCH. Both calculations yield similar structures, a ground state rotational band, a quasi-β- and a quasi-γ-band. The results are in good agreement with each other and with the data. They settle the important role of triaxiality, despite the fact that in the mean-field energy surface the triaxial states are only saddle points as shown in Figure 3(a). PNP does not change the situation very much. Only in the case of 3DAMP (Figure 3(d)) this ridge disappears and a shallow triaxial minimum de-

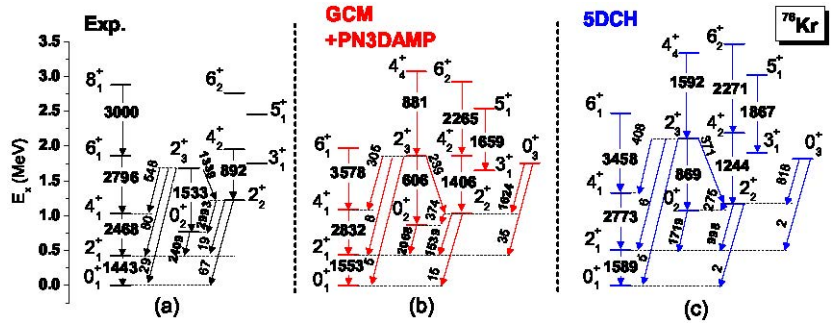

Figure 4. (Color online) Low-lying spectra and $B(E2)$ values (in $e^2\text{fm}^4$) of ^{76}Kr. Results from the full relativistic GCM calculation with PNP and 3DAMP (b) are compared with 5DCH results (c) and with experimental data (a) from Ref. [37] from Ref. [13].

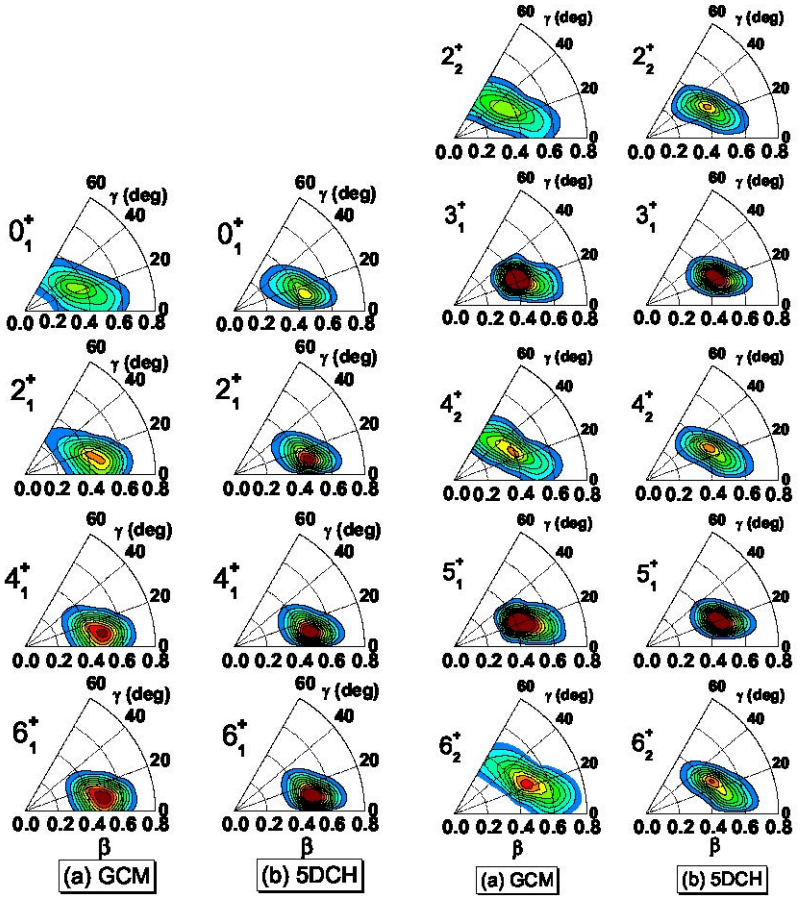

Figure 5. (Color online) Square of the collective wave functions in the (β, γ) plane for the ground state (left two panels) and for the quasi γ (right two panels) band of ^{76}Kr calculated (a) by full GCM+PNDAMP and (b) by 5DCH (from Ref. [13]).

velops. The 5DCH method uses the unprojected energy surface of (Figure 3(b)). The fact that its spectrum is still rather close to the full GCM spectrum with 3DAMP must therefore depend on the behavior of the mass parameters. As usual the 5DCH spectrum is stretched as compared to the data. This has its origin in the fact that the cranking-inertia parameters have been used in the 5DCH, where the residual interactions introducing time-odd components are neglected [38].

In Figure 5 we compare the square of the collective wave functions, i.e. the probability densities obtained from full GCM+PN3DAMP calculations with those of 5DCH results for the ground state band and for the quasi-γ-band in Figure 4. The left two panels show the ground state band. Triaxial configurations dom-

inate for all angular momenta, in general agreement with the structure of the energy surfaces given in Figure 3. With increasing angular momentum we find a very close agreement for the wave functions in both models.

The quasi-γ-band in Figure 5 shows again a very similar behavior for the GCM and for the 5DCH calculations. For even angular momenta the probability is distributed over a narrow region of β-values and a rather wide region of γ-values in both cases. On the contrary the distributions for odd I-values are sharply peaked at $\beta \approx 0.4$ and $\gamma \approx 20^\circ$. A similar strong staggering is also observed in the spectrum in Figure 4.

5 Conclusions

We have studied two fully microscopic methods for a description of shape transitions in nuclei. Both are based on relativistic density functionals beyond the mean field level. The GCM method is fully microscopic. It takes into account fluctuations and correlations resulting from the restoration of broken symmetries in the DFT wave functions. It suffers, however, from the fact that time reversal is not taken into account in a consistent way and from its numerical complexity excluding at the moment fully triaxial applications in heavy nuclei. The 5DCH, on the other hand, is extremely simple. In principle it contains the proper inertia parameters, which are however very difficult to calculate. The results of an extensive benchmark test shows that both methods lead up to small details equivalent results. This opens the way for successful calculations in heavy nuclei in the framework of a collective Hamiltonian. Both methods suffer from the fact, that the coordinates are given from outside, rather than determined in a self-consistently way.

Acknowledgments

I am grateful to my collaborators G. A. Lalazissis, Z. P. Li, J. Meng, T. Nikšić, D. Vretenar, J. M. Yao for valuable contributions and discussions. Support is also acknowledged from the DFG Cluster of Excellence "Origin and Structure of the Universe" (www.universe-cluster.de).

References

[1] F. Iachello (2001) *Phys. Rev. Lett*. **87** 052502.
[2] R.F. Casten and N.V. Zamfir (2001) *Phys. Rev. Lett*. **87** 052503.
[3] G.A. Lalazissis, P. Ring, and D. Vretenar, Eds. (2004) *Lecture Notes in Physics*, Springer-Verlag, Heidelberg, Vol. 641.
[4] T.D. Cohen, R.J. Furnstahl, and D.K. Griegel (1992) *Phys. Rev. C* **45** 1881.
[5] S.E. Agbemava, A.V. Afanasjev, D. Ray, and P. Ring (2014) *Phys. Rev. C* **89** 054320.

[6] T. Niksic, D. Vretenar, G.A. Lalazissis, and P. Ring (2007) *Phys. Rev. Lett*. **99** 092502.
[7] J.M. Yao, J. Meng, P. Ring, and D.P. Arteaga (2009) *Phys. Rev. C* **79** 044312.
[8] T. Niksic, D. Vretenar, and P. Ring (2011) *Prog. Part. Nucl. Phys*. **66** 519.
[9] T. Bürvenich *et al.* (2002) *Phys. Rev. C* **65** 044308.
[10] P.W. Zhao, Z.P. Li, J.M. Yao, and J. Meng (2010) *Phys. Rev. C* **82** 054319.
[11] T. Niksic, D. Vretenar, and P. Ring (2006) *Phys. Rev. C* **74** 064309.
[12] J.M. Yao, J. Meng, P. Ring, and D. Vretenar (2010) *Phys. Rev. C* **81** 044311.
[13] J.M. Yao, K. Hagino, Z.P. Li, J. Meng, and P. Ring (2014) *Phys. Rev. C* **89** 054306.
[14] E.F. Zhou, J. Yao, J. Meng, and P. Ring (2015) arXiv [nucl-th]1510.05232.
[15] D.L. Hill and J.A. Wheeler (1953) *Phys. Rev*. **89** 1102.
[16] P. Ring and P. Schuck (1980) *The Nuclear Many-Body Problem*, Springer-Verlag, Berlin.
[17] P. Bonche, J. Dobaczewski, H. Flocard, and P.-H. Heenen (1991) *Nucl. Phys. A* **530** 149.
[18] P.-H. Heenen, P. Bonche, J. Dobaczewski, H. Flocard, and J. Meyer (1993) *Nucl. Phys. A* **561** 367.
[19] M. Bender and P.-H. Heenen (2008) *Phys. Rev. C* **78** 024309.
[20] T.R. Rodríguez and J.L. Egido (2010) *Phys. Rev. C* **81** 064323.
[21] J.J. Griffin and J.A. Wheeler (1957) *Phys. Rev.* **108** 311.
[22] R. Krücken *et al.* (2002) *Phys. Rev. Lett.* **88** 232501.
[23] B. Giraud and B. Grammaticos (1974) *Nucl. Phys. A* **233** 373.
[24] M. Baranger and M. Veneroni (1978) *Ann. Phys. (N.Y.)* **114** 123.
[25] A. Bohr (1952) *Mat. Fys. Medd. Dan. Vid. Selsk*. **26** No 14.
[26] A. Bohr and B.R. Mottelson (1975) *Nuclear Structure Volume II: Nuclear Deformation*, W. A. Benjamin, Inc., Reading, Mass.
[27] J. Libert, M. Girod, and J.-P. Delaroche (1999) *Phys. Rev. C* **60** 054301.
[28] T. Niksic, Z. P. Li, D. Vretenar, L. Prochniak, J. Meng, and P. Ring (2009) *Phys. Rev. C* **79** 034303.
[29] P.K. Haff and L. Wilets (1973) *Phys. Rev. C* **7** 951.
[30] B. Banerjee and D.M. Brink (1973) *Z. Phys. A* **258** 46.
[31] T. Une, A. Ikeda, and N. Onishi (1976) *Prog. Theor. Phys*. **55** 498.
[32] M. Baranger and K. Kumar (1968) *Nucl. Phys. A* **122** 241.
[33] K. Goeke and P.-G. Reinhard (1978) *Ann. Phys. (N.Y.)* **112** 328.
[34] P.-G. Reinhard and K. Goeke (1987) *Rep. Prog. Phys*. **50** 1.
[35] Z.P. Li, T. Nikšić, D. Vretenar, J. Meng, G.A. Lalazissis, and P. Ring (2009) *Phys. Rev. C* **79** 054301.
[36] A. Hayashi, K. Hara, and P. Ring (1984) *Phys. Rev. Lett*. **53** 337.
[37] E. Clément *et al.* (2007) *Phys. Rev. C* **75** 054313.
[38] Z. Li, T. Niksic, P. Ring, D. Vretenar, J. Yao, and J. Meng (2012) *Phys. Rev. C* **86** 034334.